The old and new Concepts of Physics
An open-dialogue journal
www.uni.lodz.pl/concepts

HEAVIEST NUCLEI: SYNTHESIS AND DECAY PROPERTIES

Yuri Oganessian
Flerov Laboratory of Nuclear Reactions (JINR)
141980 Dubna, Moscow region, Russia.
e-mail: oganessian@jinr.ru

(Received 8 June 2008; accepted 15 June 2008)

1 Introduction

A problem of possible existence of the "islands of stability" in the region of very heavy (superheavy) elements has long been the subject of intensive discussions. The interest in this problem is linked with determining the limit of nuclear mass existence, predicted by calculation on the basis of various theoretical models. One important consequence of these calculations [1-8] was the disclosure of a significant gap in the spectrum of low lying levels in the region of deformed nuclei around N = 162 (deformed shell) and hypothetical superheavy nuclei, viz. a new (following N = 126) closed spherical neutron shell N = 184. It was also shown that the considerable variations of the binding energy of spherical nuclei were due to the nuclear shells, and that shell effects might be present also in deformed "magic nuclei" (deformed shells). And finally, at further and quite significant increase of the deformation

DOI: 10.2478/v10005-007-0046-3

arising in fission, *the shell effects continued to play an important role* in defining the potential energy and the nuclear inertial masses. Other, purely microscopic self-consistent approaches to the description of nuclear binding energies, also predict significant increase of the binding energy of heavy nuclei at $N \approx 162$ and N = 184. The theoretical predictions for the new shells, which in fact are not too far from the well established region of the actinides (it is a question of nuclei with mass $\approx 280 - 300$), push far away the limits of nuclear masses and extend the region of existing elements at least as far as $Z \sim 120$ and even more

Of main interest to us are the basic consequences of these models from the point of view of their experimental verification, and this is the main purpose of the present paper. The remarkable success in the past few years achieved in the synthesis of heavy nuclei in cold fusion reactions are related basically to isotopes in the vicinity of the N = 162 shell, mainly at $N < 162$ [9]. The decay properties (*alpha*-decay energies and half-lives, as well as spontaneous fission half-lives) of practically all synthesized nuclei up to the heaviest one ($^{277}112$) are well explained by model calculations reflecting the effect of the deformed shells Z = 108 and N = 162. But in order to probe the effect of the next, spherical shells, which influence a much wider charge and mass region of heavier nuclei, it is necessary to synthesize nuclei with $Z \geq 114$ and $N \geq 172$ This is hard to achieve in cold fusion reactions. One of the key questions pertains to the production of new "magic" nuclei in heavy-ion induced reactions.

2 Reactions of Synthesis

It has been shown also that when the two magic nuclei ^{208}Pb and ^{48}Ca fuse the maximum cross sections for evaporation residues are reached with low excitation energy (cold fusion) and small number of evaporated neutrons ($x = 1 - 3$) [10] Since 1974 the cold fusion reactions ^{208}Pb, ^{209}Bi + massive projectile ($Ap \geq 50$) have been used in the synthesis of the heaviest elements. When the projectile becomes more and more heavy, the excitation energy of the compound nuclei decreases (down to $E_x \approx 15 - 10MeV$) and the transition to the ground state takes place by the emission of only one neutron and γ-rays [11-13]. As a result, the survivability of the compound nucleus

$P_{xn}(E_x)$ significantly increases, this being the main advantage of the cold fusion reactions.

Another peculiarity of cold fusion reactions of the nuclei ^{208}Pb or ^{209}Bi with stable isotopes from ^{50}Ti to ^{70}Zn as projectiles lead to the formation of compound nuclei with small neutron excess. The EVRs are some 10-15 mass units shifted from the β-stability line. This, in turn, leads to a considerable decrease in their half-lives. Finally, in cold fusion reactions the six heaviest elements with $Z = 107 - 112$ were synthesized (see also RIKEN experiment on the synthesis of element 113 [14]). As can be seen from Fig. 1a, the cross section $\sigma_{1n}(Z_{CN})$ of the main channel of the synthesis reaction exponentially decreases with the increase of ZCN: When Z_{CN} changes from 102 to 113 the cross section decreases by almost a factor of 10^7. The observed strong decrease in the cross section with the increase of Z_{CN} in cold fusion is evidence that strong obstacles arise on the way of formation of the cold compound nucleus itself.

Transport models, describing the stage of collective motion in different assumptions about the dynamical properties of the nuclear system, indicate a strong decrease of fusion probability (P_{dyn}) with the increase of the proton number.

In order to decrease the factors hindering fusion, it is desirable to make use of more asymmetric reactions, and to obtain an increase in the neutron number of the EVRs by using neutron-rich isotopes both target and projectile nuclei with maximum neutron excess. As target material, it is reasonable to use neutron-rich isotopes of the actinides (Act.), such as ^{244}Pu, ^{248}Cm and ^{249}Cf, produced in high-flux reactors and thus having largest neutron excess. Among the projectiles, undoubted advantage has the doubly magic nucleus of the rare isotope ^{48}Ca. The compound nucleus $^{292}114$, produced, for example, in the fusion of ^{244}Pu and ^{48}Ca, acquires 8 additional neutrons compared to the case of the $^{208}Pb + ^{76}Ge$ cold fusion reaction.

These 8 neutrons, as will be shown below, play a key role in the production and the decay properties of superheavy nuclei. Compared to the cold fusion reaction $^{208}Pb + ^{76}Ge(Z_P Z_T = 2624)$, the Coulomb repulsion in the reaction $^{244}Pu + ^{48}Ca(Z_P Z_T = 1880)$ decreases by almost 40%, which, in turn, should lead to the decrease of the factors hindering the formation of a compound nucleus. On the other hand, due to the magic structure of ^{48}Ca, the excitation energy at the

Coulomb barrier E_x^{min} of the compound nucleus $^{292}114$ amounts to approximately 30 MeV, a value by 10-15 MeV lower than in typical hot fusion reactions induced by lighter projectiles.

The last stage – the survival of the compound nucleus – is the decisive one in the given method of synthesis of the heaviest nuclei. The estimations of E_x^{min} and the following experiments, aimed to measure the excitation functions for evaporation products, have shown that the compound nuclei with Z_{CN} = 112-118, may attain excitation energy from 30 to 55 MeV. This energy will be released by a cascade emission of 2 to 5 neutrons (the evaporation of charged particles is significantly less probable) and γ-rays. Indeed the excitation functions correspond to the evaporation mainly of 3 or 4 neutrons from the excited nucleus, the maximum cross sections for evaporation residues are observed at $E_x \approx 40 MeV$ [15] (hot fusion). The cross sections of nuclei with Z = 102-110, produced in the 4n-evaporation channel of the fusion reactions Act. + ^{22}Ne, ^{26}Mg, $^{36}S(5n)$, are presented in Fig. 1b (the neutron number of the corresponding compound nuclei is shown on the horizontal axis). Since there is no significant hindrance for fusion in such mass-asymmetric reactions ($Z_P \dot{Z}_T = 920 - 1500$), the strong decrease in the cross section σ_{4n} is connected mainly with the survivability of the nuclei. The relatively high production cross section of isotopes with $Z \leq 105$ is a consequence of the high fission barrier, which is almost completely determined by the shell effect of the two closed neutron shells N = 152 and N = 162. At neutron numbers $N_{CN} > 162$, see Fig. 1b (lower graph), the fission probability significantly increases with the decrease of B_f.

However, if the predictions of the theoretical models (see above) about the existence of the next closed shell N = 184 is justified, the fission barrier height will again increase when advancing to the region where $N_{CN} \geq 174$ and $Z_{CN} \geq 112$. In turn, the nuclear survivability will increase too and as a result, one can expect even a rise in the σ_{EVR} for heavy nuclei with large neutron excess. Indeed, as can be seen from the experimental data presented in Fig. 1b, when increasing the number of neutrons from $N_{CN} = 169(^{233}U + {}^{48}Ca)$ to $N_{CN} = 172(^{237}Np + {}^{48}Ca)$ and then to $N_{CN} = 178 - 180(^{244}Pu, {}^{248}Cm + {}^{48}Ca)$, σ_{EVR} grows by more than one order of magnitude. For this reason, the observed increase in the survivability of the excited nuclei with neutron number appears to be, to our

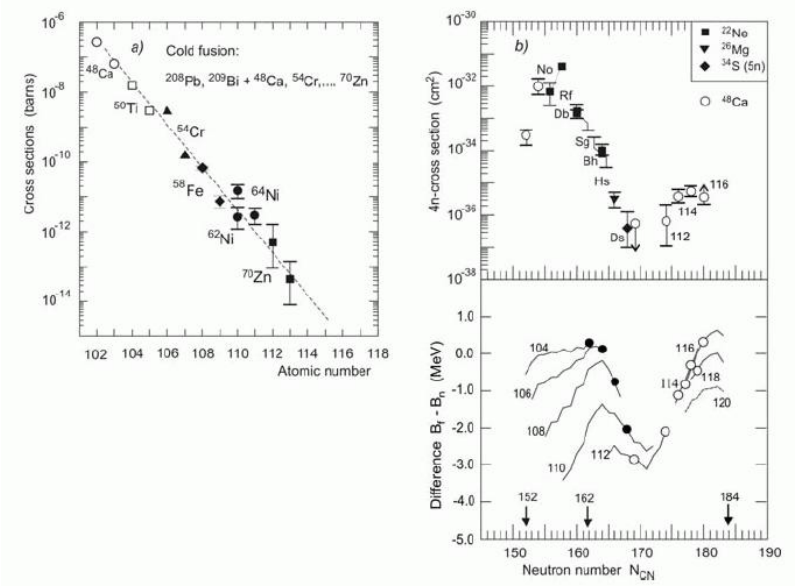

Figure 1: a) Maximal cross sections of the 1n-evaporation channel in cold fusion reactions. b) Upper panel: Experimental cross sections at the maximum of 4n-evaporation channels in hot fusion reactions. Lower panel: Calculated values of (B_n - B_f) for isotopes of elements 102-120 with different neutron number.

opinion, evidence for the existence of the closed neutron shell in the region of $N \geq 180$.

3 Setting the Experiments

The Gas-Filled Recoil Separator (DGFRS) used in the experiments with ^{48}Ca-projectiles is schematically presented in Fig. 2. The calculated and measured in the test experiments transmission efficiency of the separator for Z = 112-118 nuclei is about 35-40%, whereas full-energy ^{48}Ca projectiles, projectile-like ions, and target-like nuclei are suppressed by factors 10^{17}, $6 \cdot 10^{14}$, and $10^4 - 10^6$, respectively.

The typical beam intensity of ^{48}Ca ions at the target was $1.0 - 1.2 p\mu A$. In the experiments, targets of actinide oxides of the highly enriched isotopes of U, Np, Pu, Am, Cm and Cf (thickness of $\approx 0.35 mg/cm^2$) were used.

EVRs passing through the separator were implanted in a 4x12-cm^2 semiconductor detector with 12 vertical position-sensitive strips. The detection efficiency of the focal-plane detector array for α-particles is 87% of 4π for detection one fission fragment - close to 100%, for two fission fragment - about 40%. For α-particles, emitted by the parent or daughter nuclei, it is possible to choose wide enough energy and time gates $\delta E_{\alpha 1}$, $\delta t_{\alpha 1}$ and $\delta E_{\alpha 2}$, $\delta t_{\alpha 2}$ and employ a special low-background detection scheme. Switching off the beam during registering the decay of the nucleus implanted into the detector allows entirely remove the background of reaction products and scattered ions. As a result, such running condition allowed detection of rare events and decay characteristics of heaviest nuclei with decay time of up to 1d and even longer [16]. The most short-lived nuclei are detected in DGFRS corresponding to $t \geq 5\mu s$. In this way, the setup allows investigation of nuclei in a wide range of half-lives . from $10^{-5}s$ to more than $10^5 s$.

From the characteristics of the DGFRS, which are given above, it follows that with a ^{48}Ca-beam intensity of $1.2 p\mu A, 0.35 mg/cm^2$ target thickness and a beam dose 510^{18} (realized for 200 hours of operation) the observation of one decay event corresponds to the production cross section of about $0.7 pb$.

4 Experimental Results

For the synthesis of superheavy nuclei at DGFRS, the fusion reactions of ^{48}Ca with target nuclei, the isotopes of U, Np, Pu, Am, Cm and Cf (nine isotopes of six actinide elements), were used. The decay chains are presented in Fig. 3. In the investigations carried out at different ^{48}Ca energies, 34 new nuclides were detected, all of them being evaporation products and their daughter nuclei in the region of $Z = 104 \div 118$ and $A = 266 \div 294$ [15-17].

Before discussing the properties of the new nuclides let us consider a problem of their mass and charge identification. In cold fusion reactions sequential -decays of neutron-deficient nuclei led to daughter

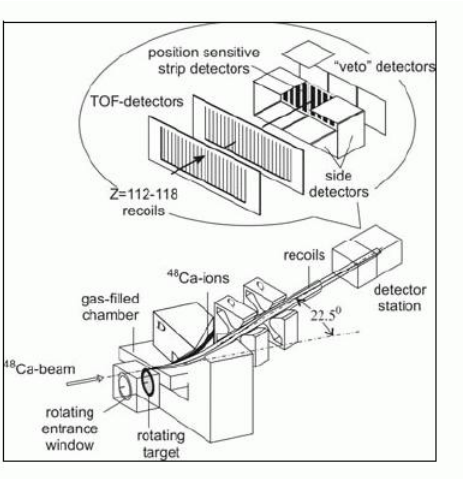

Figure 2: Layout of the Gas-filled Recoil Separator.

products in a known nuclear region. Identification of mass and charge number of a new nuclide is determined here by the decay properties of the known daughter nucleus and by establishing correlations in sequential α-transitions leading to its formation. Evaporation products of the reaction Act. $+^{48}Ca$ have a larger neutron number; their sequential -decays take place among unknown nuclei and are terminated by spontaneous fission.

In this case some additional measurements are needed. The setting of independent experiments aimed at the registration of nuclei in the decay chains from the DGFRS is most preferable in the Act. $+^{48}Ca$ reaction.

Here it is worthwhile to mention that as a result of sequential α-decays, in the long chains of odd nuclei long-lived neutron-rich isotopes of elements 104 and 105 are formed, which can be separated from a huge amount of the reaction products by radiochemical methods and identified their atomic number.

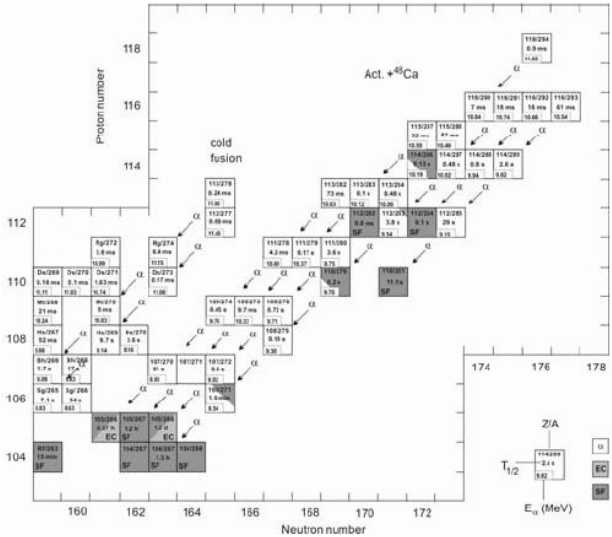

Figure 3: Chart of the heaviest nuclides. The squares contain the half-lives (without errors) and the maximum α-transition energy (E_α in MeV).

5 Chemical Experiments

The experimental method used is demonstrated by the example of the synthesis of elements 113 and 115 in the reaction $^{243}Am+^{48}Ca$ [16]. The evaporation of three neutrons and the emission of the γ-rays by the compound nuclei of element 115, produced in the fusion reaction, lead to the formation in the ground state of the odd-odd nuclide with 115 protons and 173 neutrons. This nuclide is the parent of a "radioactive family" consisting of the $Z = 115 - \alpha - 113 - \alpha - 111 - \alpha - 109 - \alpha - 107 - \alpha - 105(SF)$ nuclei, formed as a result of the five consecutive emissions of α-particles, and terminated by SF of the Db isotope (Z = 105). Due to the long lifetime, the atoms of element 105 can be separated by a classical off-line radiochemical method of ion-exchange chromatography, with the consequent measurement of their decay by SF. In eight identical experiments $^{243}Am+^{48}Ca$, after

chemical separation of Nb-Ta fraction, 15 SF events were detected with $T_{1/2} \sim 1$ day [18]. It was shown that the SF observed in the decay of the $^{288}115$ nucleus comes from an element, which is a representative of the 5th group of Periodic Table of the Elements. The chemistry experiment gives an independent and unambiguous identification of the atomic number of the final nucleus (Z = 105) and at the same time the atomic numbers of all nuclides in the fully correlated chain of the decay of the parent nucleus $^{288}115$.

The method of chemical identification of the ^{268}Db can be applied also for another SF-nuclide, viz. ^{267}Rf ($T_{SF} \approx 1.3h$), which terminates the long decay sequence of even-Z nuclei:

$$^{291}116(\alpha) \rightarrow {}^{287}114(\alpha) \rightarrow {}^{283}112(\alpha) \rightarrow {}^{279}110(SF/\alpha) \rightarrow {}^{275}108(\alpha) \rightarrow$$
$$\rightarrow {}^{271}106(SF/\alpha) \rightarrow {}^{271}104(SF),$$

see Fig. 3. Unfortunately, the high probability for spontaneous fission of the preceding nuclei $^{279}110$ and $^{271}106$ reduces by more than one order of magnitude the effective production cross section of this nucleus. In order to surpass this limitation, it is reasonable to study heavier nuclei with $Z > 110$ applying express radiochemical techniques. The most suitable this purpose are the odd isotopes of element 112 : $^{283}112(T_{1/2} \approx 4s)$ and $^{285}112(T_{1/2} \approx 30s)$, undergoing α-SF decay.

According to the atomic configuration in the ground state, element 112 should belong to the 12^{th} group of the Periodic Table as a heavier homologue of Hg, Cd and Zn. To what extent element 112 is a homologue of Hg depends on the so-called relativistic effect in the electronic structure of the superheavy atom. According to some relativistic calculations, the chemical behaviour of element 112 (and other elements with a larger atomic number) will somewhat differ from that of its light homologue. The predictions claim an increased chemical stability and a noble-gas like inertness similar to radon [19]. On the contrary, other calculations of the full electronic structure of the element-112 atom predicted its chemical behaviour like a noble transition metal [20]. Recently, relativistic density functional calculations of the stability of molecules between element 112 and a noble metal (interaction of element 112 with gold clusters) predicted a behaviour close to Hg [21]. Will element 112 as actively as Hg interact with Au or just the opposite will be closer to the chemically neu-

tral Rn? Both characteristics the high volatility and the ability to form inter-metallic compounds, defined the experimental setup for the chemical identification of element 112.

The reaction $^{242}Pu(^{48}Ca, 3n)^{287}114 - \alpha \rightarrow {}^{283}112$ was used to produce the isotope $^{283}112$. The recoil nuclei: $49s$-$^{185}Hg, 3.6s$-$^{283}112$ and 4s-^{219}Rn isotopes leaving the ^{242}Pu-target ($1.4mg/cm^2 + 15\mu g/cm^2$ of ^{nat}Nd) stopped in a high-purity He/Ar gas medium: and were transported to the detectors by means of an 8m-capillary tube.

The setup COLD [22] consists of 32 pairs detectors, about $1cm^2$ each, placed one opposite the other with a 1.5 mm gap in between, through which the He/Ar gas flows. One of the detectors of each pair was covered with a 30-50 nm gold layer. The temperature gradient along the whole length of the detectors spanned a range from -24^0C to -184^0C in the first experiment, from $+35^0C$ to -180^0C in the second and from $+32^0C$ to -164^0C in third one. The other experimental conditions in which the temperature and transport rate of recoil nuclei was changed are shown in Fig. 4 [23]. Energy resolution for decay α-particles amounted to 120 keV. The SF fission fragment energy was calibrated using a thin ^{248}Cm source. As it was expected, only nuclei with high volatility were transported to the detectors. It was shown that all Hg atoms are registered by the first detectors with the Au coating. This can be explained by the strong adsorption on the detector Au-surface, which is due to the chemical reaction leading to the production of the (HgAu) compound. On the contrary, the decay of the chemically neutral Rn atoms is observed in the region of the last detectors, which are at the lowest temperatures, consistently with the adsorption enthalpy. In these conditions, the atoms of element 112 must be between these two extreme cases.

All five registered cases of the isotope $^{283}112$ all measured α-SF decay parameters coincide with the data obtained at the DGFRS. In four cases out of five, absorption of element 112 atoms occurred at the Au-surface of the detector (one event in the ice layer). The obtained distributions of events along the detectors give evidence on the formation of compound (112Au) and point to the high volatility of element 112.

Finally, at the GSI, at the separator SHIP an experiment on the synthesis of element 112 in the reaction $^{238}U(^{48}Ca, 3n)^{283}112$ have been recently re-conducted. The decay properties of this nuclide are

in full agreement with the data obtained at the DGFRS and with the chemical tests described above. A detailed presentation of these experimental results is given in [24].

The identification of the atomic numbers of the nuclides was performed by:

- the mechanism of fusion reactions (excitation functions and cross bombardments ensuring variation of the proton and neutron numbers of the compound nucleus);

- the decay properties of the nuclei in the decay sequences (half-lives T_α and α-decay energies Q_α of even-even (and for many even-odd) isotopes; see Fig.4).

- the radiochemical identification of the atomic number of the nuclides ^{268}Db and $^{283}112$ links of the decay chains of the parent nuclei: $^{288}115$ and $^{291}116$. All methods give the same identification of the atomic number of the synthesized nuclei. When the atomic numbers of the parent nuclei are determined (showing that they are the products of xn-evaporation channels)

All methods give the same identification of the atomic number of the synthesized nuclei. When the atomic numbers of the parent nuclei are determined (showing that they are the products of xn-evaporation channels), the identification of the mass of an isotope comes to the quantification of evaporated neutrons at various excitation energies. This is achieved:

- by means of the measured excitation functions ensuring variation of the neutron number in the compound nucleus;

- by producing the same nuclei in different ways: as evaporation residues and as α-decay products of heavier nuclei.

The adjoining four isotopes of the elements with Z = 112, 114 and 116, genetically connected with the daughter nuclei by consecutive - decays give a self-consistent picture of the atomic and mass numbers of all nuclides, synthesized in the ^{48}Ca-induced experiments. Further verification of the identification of the mass number of the isotopes follows from the decay properties. Because of the high suppression

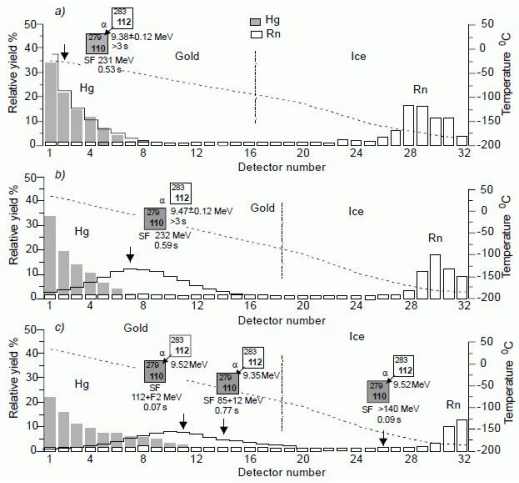

Figure 4: Thermo-chromatographic deposition patterns ^{185}Hg, ^{219}Rn, and $^{283}112$ in the COLD dependent on experimental parameters: ^{185}Hg (grey bars,), ^{219}Rn (white bars) and $^{283}112$ (black arrows); the temperature gradient is shown (black dashed line, right hand axis); a) gas flow 860 ml/min, temperature gradient from -24^0C to -184^0C; b) gas flow 890 ml/min, temperature gradient from 35C to -180C; c) gas flow 1500 ml/min, temperature gradient from 32^0C to -164^0C; the beginning ice coverage of the detectors at -95^0C is indicated by vertical dash-dotted line. Solid line - Monte-Carlo simulation to evaluate the enthalpy on gold surface of 112 elements.

of spontaneous fission of nuclei with odd neutron numbers, their decay chains are longer and the total decay time is with odd neutron numbers, their decay chains are longer and the total decay time is noticeably higher than in the neighbouring even-N isotopes (see chains on the Fig.3).

6 Decay Properties of Superheavy Nuclei Alpha Decay

As can be seen from Fig. 3, the odd isotopes of element 112 and all isotopes (even and odd) with $Z \geq 113$ predominantly undergo α-decay. As known from the theory of α-decay, the probability of decay (or the half-life T_α) for allowed transitions are directly connected to the decay energy Q_α and the atomic number of the nucleus.

The experimental values obtained earlier in hot and cold fusion reactions and belonging to the α-decay of even-even nuclei with $100 \leq Z \leq 110$ with new data for all isotopes with even proton numbers from Z = 106 to 118, produced in ^{48}Ca-induced reactions, are shown in Fig. 5. The experimental values Q_α(exp) and T_α(exp) shows steep raise of the T_α with increase the neutron number in heaviest nuclei. They can be used for the calculation of the atomic numbers of nuclei comprising the chains of correlated decays. For example the probability that the consecutive α-transitions observed in the ^{245}Cm, $^{248}Cm + {}^{48}Ca$ reaction take place in the nuclei with atomic numbers $116 \rightarrow 114 \rightarrow 112 \rightarrow 110$ amounts to 0.992.

The values of Q_α(th), obtained in the framework of the MM-model in the version of [25] for the isotopes of all elements with even atomic numbers from Z = 100 to 118 and with odd atomic numbers from Z = 103 to 115, are presented in Fig. 5a and Fig. 5b, respectively. The predicted Q_α(th) values for the heaviest nuclei, observed in our experiments are systematically larger than the experimental data.

At the same time, the trends of the predictions are in good agreement for the 23 nuclides with Z = 106-118 and N = 165-177. The trend of the $Q_\alpha(N)$ systematics, predicted by theory and confirmed by experimental data can be considered as *direct evidence for the deformed neutron shell closure at* N = 162. The comparison of Q_α(exp) with the values Q_α(th), calculated within the Skyrme-Hartree-Fock-Bogoliubov (HFB) and the Relativistic Mean Field models (RMF), was carried out, too.

In the HFB model a better agreement is obtained with masses from [26] calculated with 18 parameters. Finally, in the RMF model the agreement between theory and experiment is the least satisfactory. But it cannot be excluded that a better agreement can be achieved in this model also by using a different set of parameters.

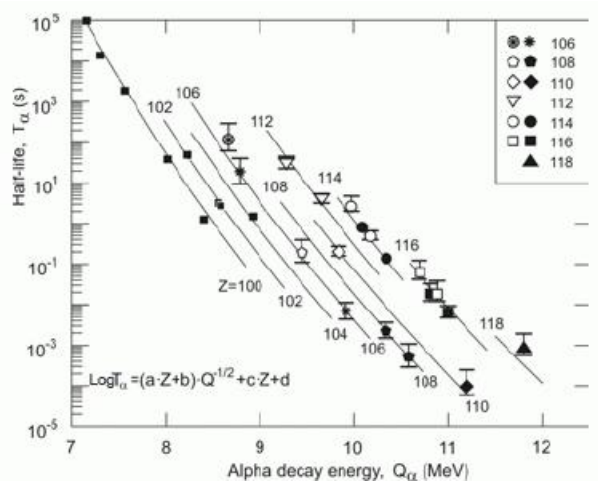

Figure 5: Half-lives T_α as a function of the α-decay energy Q_α for nuclei with even atomic numbers $Z \geq 100$ (indicated in the figure). The solid lines represent calculations using the Viola-Seaborg formula (given in the figure). The black symbols denote even-even isotopes, the open symbols . even-odd.

As a whole, the measured values of Q_α(exp) are in agreement with theory, because the model calculations do not claim to be more precise in determining Q_α(N) than 0.4-0.6 MeV. We must recall, that all three models predict the same spherical neutron shell at N = 184, but different proton shells, Z = 114 (MM) and Z = 120, 124 or 126 (HFB, RMF). Yet, all describe the experimental data equally well. Such insensitivity with respect to the various models in this region of Z and N can be explained either by the remoteness of the nuclei under consideration from the closed shell at N = 184 or by the weaker influence of the proton shells at Z = 114 or higher, compared to that of the neutron shell at N = 184.

7 Spontaneous Fission

For 8 out of the 34 synthesized nuclei spontaneous fission is the predominant mode of decay. In two more nuclei, ^{271}Sg and $^{286}114$,

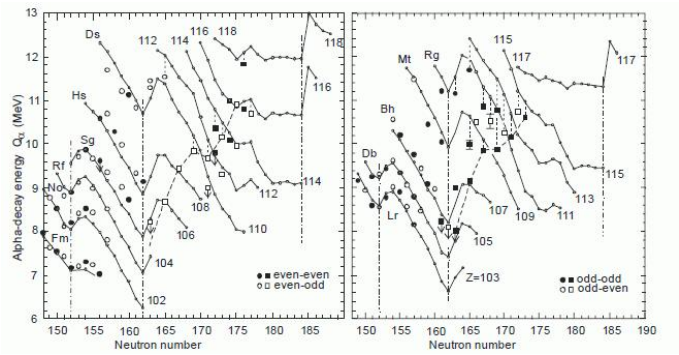

Figure 6: Alpha-decay energy vs. neutron number for: a) the isotopes of even-Z elements with $Z \geq 100$, b) isotopes of odd-Z elements with $Z \geq 103$. Squares correspond to the nuclei, produced in ^{48}Ca-induced reactions. Dashed lines are long sequences of correlated decays of the nuclei $^{288}115$ and $^{291}116$. The solid lines are Q_α(th), calculated in the MM-model.

spontaneous fission competes with α-decay. For the remaining nuclides spontaneous fission was not observed. The partial SF half-lives of nuclei with $N \geq 163$, produced in fusion reactions with ^{48}Ca, together with the half-lives of SF-nuclides with $N \leq 160$, are shown in Fig. 6. Four isotopes of element 112 with N = 170-173 are located in a region, where a steep rise of $T_{SF}(N)$ is expected. Indeed, in the even-even isotopes $^{282}112$ and $^{284}112$ the difference of two neutrons increases the partial half-life T_{SF} by two orders of magnitude. The neighbouring odd isotopes $^{283}112$ and $^{285}112$ undergo α-decay. For them, only lower limits of T_{SF} can be determined (shown in the figure). Such a picture is observed also for the even-even isotopes of element 114: the additional two neutrons in the nucleus $^{286}114$ ($T_{SF} \approx 0.13s$) lead to significant increase of the stability relative to spontaneous fission. It is significant that the rise of stability relative

to spontaneous fission is observed for the nuclei are by 10-12 neutrons away from the closed neutron shell N = 184.

On moving to the nuclei with $Z < 110$ and $N < 170$ the probability for spontaneous fission decreases again when the close deformed shell N = 162 is approached. The stabilizing effect of the N = 162 shell manifests itself in the properties of the even-even isotopes of Rf, Sg and Hs with $N \leq 160$, which, as seen from Fig.7, are well described by the mentioned model calculations. The odd SF-isotopes with Z = 104-110, produced in the ^{48}Ca- induced reactions, are located in the transition region, where the larger the neutron number, the smaller the effect of the N = 162 shell. In this region, the N = 184 shell comes into effect. Such a behaviour of T_{SF}(exp) as a function of Z and N correlates with the SHE fission barrier heights and has been predicted by all models: MM, HFB and RMF. For the isotopes of element 115, due to the strong hindrances to spontaneous fission of nuclei with odd proton (or/and neutron) number, α-decay predominates as far as the N = 162 shell, where, similarly to the previous case, the sequences terminates by spontaneous fission

8 Conclusion

Decay properties of the nuclei obtained in Act. $+^{48}Ca$ reactions show that the basic theoretical concept on the existence of closed shells in the region of the hypothetical superheavy elements and their decisive role in defining the limits of nuclear mass has received its experimental confirmation.

The experiments were carried out at the Flerov Laboratory of Nuclear Reactions (JINR, Dubna) in collaboration with the Analytical and Radiochemical Division of the Lawrence Livermore National Laboratory (LLNL, Livermore); the experiments on the chemical identification of the isotopes ^{268}Db and $^{283}112$ within the collaboration: Paul Scherrer Institute (PSI, Villigen) - Department for Chemistry and Biochemistry of the University of Bern FLNR (Dubna) - LLNL (Livermore) - Institute of Electronic Technology (IET, Warsaw) with the participation of Dr. M. Hussonois from the Institute of Nuclear Physics (IPN, Orsay).

9 Acknowledgments

It is my pleasure to convey my gratitude to my colleagues and coauthors of the majority of original publications for their hard work

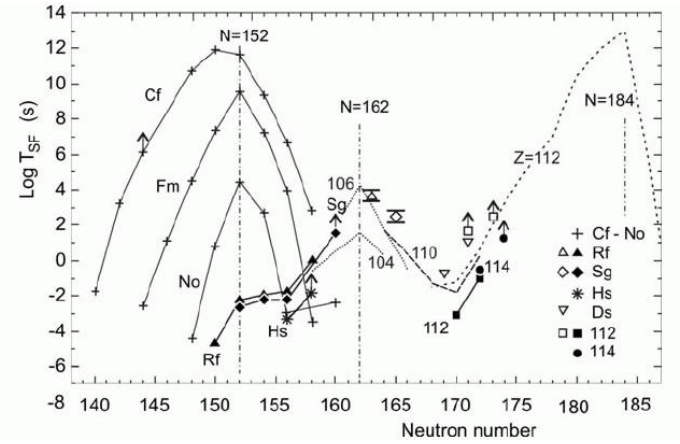

Figure 7: Partial half-lives for spontaneous fission T_{SF} vs. N for nuclei with even Z = 98-114. Solid symbols and crosses denote even-even nuclei, open symbols even-odd. Solid lines are drawn through the experimental points of even-even nuclei, the dashed lines calculated $T_{SF}(th)$.

and active participation in the experimental programme on the synthesis and study of the properties of superheavy elements.

It is my duty to thank Profs. W. Greiner, S. Hoffman, M. G. Itkis, G. Muenzenberg, A. Sobiczewski, W. J. Światecki, V. V. Pashkevich, K. Siwek-Wilczyńska, J. Wilczyński and H .W. Gäeggeler, as well as Dr. V. K. Utyonkov, Profs. V. I. Zagrebaev and S. N. Dmitriev. With them I had interesting and fruitful discussions.

References

[1] M. Brack, et al., Rev. Mod. Phys. 44 (1972) 320. 15

[2] A. Sobiczewski, F. A. Gareev and B. N. Kalinkin, Phys Lett. 22 (1966) 500.

[3] H. Meldner, Ark. Fys 36 (1967) 593.

[4] U. Mosel and W. Greiner, Z. Phys. 222 (1969) 261.

[5] P. Möller and J. R. Nix, J. Phys. G 20 (1994) 1681.

[6] W. Greiner, Int. J. Mod. Phys. E 5 (1995).

[7] A. Sobiczewski, Phys. Part. Nucl. 25 (1994) 119.

[8] R. Smolańczuk, J. Skalski and A. Sobiczewski, Phys. Rev. C52 (1995) 1871.

[9] S. Hofmann, Rep. Prog. Phys., 61 (1998) 639.

[10] G. N. Flerov, et al., Nucl. Phys. A 267, (1976) 359.

[11] P. Armbruster, Annu. Rev. Nucl. Part. Sci., 35 (1985) 135.

[12] G. Munzenberg, Rep. Prog. Phys. 51 (1988) 57.

[13] S. Hofmann and G. Munzenberg, Rev. Mod. Phys. 72 (2000) 733.

[14] K. Morita et al., J. Phys. Soc. Jpn, 73 (2004) 2593.

[15] Yu.Ts. Oganessian, et al., Phys. Rev. C 69, 054607(2004). Phys. Rev. C 70, 064609(2004).

[16] Yu.Ts. Oganessian, et al., Phys. Rev. C 69, 021601(R) (2004).

[17] Yu. Ts. Oganessian, et al., Phys. Rev. Lett. 85, (1999) 3154; Phys. Rev. C62, (2000), 041604 (R); Yad. Fiz. 63, (2000) 1769 [Phys. At. Nucl. 63, (2000) 1679]; Phys. Rev.C 63, (2001) 011301(R). Nucl. Phys. (2004) A 734, 109. Phys. Rev. C 72, (2005) 034611; Phys. Rev. C74, (2006) 044602.

[18] S.N. Dmitriev, et al., Mendeleev Commun. 1 (2005) 1.

[19] K. S. Pitzer, J. Chem. Phys. 63 (1975) 1032.

[20] E. Eliav et al., Phys. Rev. A 52, (1995) 2765; M. Seth, P. Schwerdtfeger, and M. Dolg , J. Chem. Phys. 106, (1997) 3623

[21] V. Pershina et al., Radiochim. Acta 94, (2006) 181.

[22] Ch. E. Düllmann et al., Nucl.Instr.Meth A479 (2002), 631; S. Soverna et al, Radiochimica Acta, 93, (2005) 1.

[23] R. Eichler et al., Nature 447, (2007) 72. Talk at the 3rd Int. Conf. on the Chemistry and Physics of the Transactinide Elements, Sept. 23-28, Davos, Switzerland.

[24] S. Hofmann et al., Eur. Phys. J. A32, (2007) 251.

[25] I. Muntian, Z. Patyk, and A. Sobiczewski, Acta Phys. Pol. B34 (2003) 2073. Phys. At.Nucl. 66, (2003) 1015.

[26] S. Goriely et al., Phys. Rev. C66, (2002) 024326.